

# Solvation Forces on Biomolecular Structures: A Comparison of Explicit Solvent and Poisson–Boltzmann Models

JASON WAGONER, NATHAN A. BAKER

*Department of Biomedical Engineering, Center for Computational Biology, Washington  
University in St. Louis, 700 S. Euclid Avenue, Campus Box 8036, St. Louis, Missouri 63110*

*Received 20 February 2004; Accepted 28 May 2004*

*DOI 10.1002/jcc.20089*

*Published online in Wiley InterScience (www.interscience.wiley.com).*

**Abstract:** Continuum electrostatics methods have become increasingly popular due to their ability to provide approximate descriptions of solvation energies and forces without expensive sampling required by explicit solvent models. In particular, the Poisson–Boltzmann equation (PBE) provides electrostatic potentials, solvation energies, and forces by modeling the solvent as a featureless, dielectric material, and the mobile ions as a continuous distribution of charge. Polar solvation forces and energies obtained from the PBE are often supplemented with simple solvent-accessible surface area (SASA) models of nonpolar solvation. Given the recent development of methods that enable the use of PBE and SASA forces in molecular dynamics simulations, it is important to determine the ability of these implicit solvent models to accurately reproduce the solvation forces of more detailed explicit solvent simulations. In this article, we compare PBE and SASA solvation forces with explicit solvent forces for several snapshots from eight trajectories of static conformations of intestinal fatty acid binding protein. The results from this comparison show that current implementations of the PBE are capable of generating polar solvation forces that correlate well with explicit solvent forces but systematically overestimate the magnitude of the interaction. However, SASA-based nonpolar forces are found to have no significant correlation with nonpolar explicit solvent forces. Nevertheless, due to the small magnitude of the nonpolar forces in the current system, a good correlation is still obtained for total solvation forces. The good correlation of implicit solvent forces with more detailed explicit solvent models is encouraging and implies that the systematic errors identified in these models could be corrected by appropriate parameterization of the force fields.

© 2004 Wiley Periodicals, Inc. J Comput Chem 25: 1623–1629, 2004

**Key words:** Poisson–Boltzmann; solvation force; solvation energy; molecular dynamics

## Introduction

Electrostatics and solvation play important roles in the structure and dynamics of biomolecules, and the computational study of such properties requires an accurate description of solvation forces and energies.<sup>1–4</sup> A number of models are currently available to compute these solvation forces, each of which offer a varying degree of microscopic detail in exchange for computational efficiency. Molecular dynamics (MD) methods, which use explicit solvent representations, are the most computationally demanding of these methods. Given the computational effort required to fully sample the vast conformational space of explicitly solvated macromolecules, the analysis of converged solvation properties using explicit solvent simulations can quickly become intractable for large systems. Continuum (or “implicit”) solvent methods, such as Poisson–Boltzmann (PB)<sup>1,5–8</sup> and Generalized Born (GB)<sup>5,9–11</sup> models, conveniently lower the computational cost by implicitly accounting for solvation effects via a

simple dielectric model. Such implicit solvent models have become increasingly popular techniques for describing biomolecular electrostatic interactions in solvent.

The PB equation (PBE) is a continuum model whereby the solvent is modeled as a featureless, dielectric continuum, and the dissolved electrolyte as a continuous charge distribution. In the context of this model, the electrostatic potential is given as the solution to a partial differential equation that can be solved using a variety of methods.<sup>12–20</sup> The PBE has been used in a number of biomolecular simulation applications, including the accurate representation of biomolecular electrostatic potentials<sup>21</sup> and energet-

**Correspondence to:** N.A. Baker; e-mail: baker@biochem.wustl.edu

Contract/grant sponsor: National Institutes of Health; contract/grant number: GM069702

Contract grant sponsor: Alfred P. Sloan Foundation

**Table 1.** Coordinate RMSD Values (Å) between the Eight Conformations Used in the Molecular Dynamics Trajectories of Static Conformations of IFABP.

Conf.	1	2	3	4	5	6	7	8
1	0	1.27	1.72	2.07	2.31	2.25	2.41	2.42
2	1.27	0	1.64	1.91	2.16	2.12	2.28	2.33
3	1.72	1.64	0	1.75	2.02	2.08	2.24	2.33
4	2.07	1.91	1.75	0	1.82	1.84	2.04	2.05
5	2.31	2.16	2.02	1.82	0	1.35	1.75	1.80
6	2.25	2.12	2.08	1.84	1.35	0	1.56	1.57
7	2.41	2.28	2.24	2.04	1.75	1.56	0	1.28
8	2.42	2.33	2.33	2.05	1.80	1.57	1.28	0

ics.<sup>22</sup> Recently, the breadth of the PB applications has been considerably extended with the introduction of methods to compute solvation forces<sup>23–28</sup> with sufficient efficiency for routine use in molecular dynamics simulations.<sup>16,23,24,27,29,30</sup> In particular, recent work by Luo and coworkers<sup>16,29</sup> has demonstrated that PB-based forces can be evaluated nearly as quickly as simpler models such as GB. Additionally, PB solvation forces and energies are routinely used to benchmark and parameterize other continuum methods, in particular, the popular GB solvation model.<sup>5,9,10,31–33</sup>

Given the numerous applications of PB calculations in biomolecular modeling, the need for accurate calculations is clearly important. However, there have been relatively few attempts to optimize atomic parameters (particularly radii) for PB applications,<sup>25,34</sup> and such optimizations have typically focused on solvation energies rather than atomic solvation forces. In this article, we compare solvation forces from explicit solvent molecular dynamics simulations of intestinal fatty acid binding protein with solvation forces determined by solution of the PB equation. This comparison quantifies the ability of continuum solvent models to reproduce explicit solvent forces, and lays the groundwork for future parameterization of atomic radii and other parameters for PB calculations. This work is similar in spirit to that of Onufriev et al.,<sup>32</sup> who compared GB and PB forces for several protein conformations from a molecular dynamics trajectory. However, given the fact that the PB (or Poisson) model is often used as the “true” solvation force for parameterizing GB calculations, it is important to have a clear understanding of the ability of PB forces to reproduce explicit solvent values.

## Methods

### Conformational Sampling

Implicit and explicit solvation forces were compared for eight conformations (coordinate RMSD values given in Table 1) of intestinal fatty acid binding protein (IFABP) obtained from a molecular dynamics trajectory starting from an NMR structure (PDB 1D 1AEL).<sup>35</sup> In particular, the conformations were obtained from conformational clustering (obtained using g\_cluster of GRO-MACS<sup>36</sup>) of a 2.5-ns trajectory of IFABP in a  $66.8 \times 64.2 \times 62.4$  Å box of TIP3P water<sup>37</sup> in the presence of 26 Na<sup>+</sup> ions and 26 Cl<sup>−</sup>

ions (~150 mM local NaCl concentration). The trajectory was simulated at constant pressure (1 atm) and temperature (300 K) using the AMBER7 software<sup>38</sup> with the AMBER94 force field,<sup>39</sup> 2-fs time steps, and SHAKE constraints.<sup>40</sup>

### Explicit Solvent Forces

As described by Roux and Simonson,<sup>35</sup> the total solvation energy of a solute in water can be decomposed into a polar term  $W^{(p)}(\mathbf{X})$  and a nonpolar term  $W^{(np)}(\mathbf{X})$  according to the formulae:

$$e^{-\beta W^{(p)}(\mathbf{X})} = \langle e^{-U_{uv}^{(p)}(\mathbf{X}, \mathbf{Y})} \rangle_p = \frac{\int e^{-\beta[U_{vv}(\mathbf{Y}) + U_{uv}^{(np)}(\mathbf{X}, \mathbf{Y}) + U_{uv}^{(p)}(\mathbf{X}, \mathbf{Y})]} d\mathbf{Y}}{\int e^{-\beta[U_{vv}(\mathbf{Y}) + U_{uv}^{(np)}(\mathbf{X}, \mathbf{Y})]} d\mathbf{Y}}$$

$$e^{-\beta W^{(np)}(\mathbf{X})} = \langle e^{-U_{uv}^{(np)}(\mathbf{X}, \mathbf{Y})} \rangle_{np} = \frac{\int e^{-\beta[U_{vv}(\mathbf{Y}) + U_{uv}^{(np)}(\mathbf{X}, \mathbf{Y})]} d\mathbf{Y}}{\int e^{-\beta U_{vv}(\mathbf{Y})} d\mathbf{Y}} \quad (1)$$

where  $\beta$  is the inverse thermal energy,  $\mathbf{X}$  represents the solute degrees of freedom,  $\mathbf{Y}$  represents the solvent degrees of freedom,  $U_{vv}(\mathbf{Y})$  is the solvent potential,  $U_{uv}^{(p)}(\mathbf{X}, \mathbf{Y})$  is the polar (electrostatic) portion of the solute–solvent potential, and  $U_{uv}^{(np)}(\mathbf{X}, \mathbf{Y})$  is the nonpolar portion of the solute–solvent potential. Differentiation with respect to the solute coordinates provides an analogous description of the solvation forces:

$$\mathbf{F}^{(p)}(\mathbf{X}) = - \frac{\partial W^{(p)}(\mathbf{X})}{\partial \mathbf{X}}$$

$$= - \left\langle \frac{\partial U_{uv}^{(p)}(\mathbf{X}, \mathbf{Y})}{\partial \mathbf{X}} + \frac{\partial U_{uv}^{(np)}(\mathbf{X}, \mathbf{Y})}{\partial \mathbf{X}} \right\rangle_p + \left\langle \frac{\partial U_{uv}^{(np)}(\mathbf{X}, \mathbf{Y})}{\partial \mathbf{X}} \right\rangle_{np}$$

$$\mathbf{F}^{(np)}(\mathbf{X}) = - \frac{\partial W^{(np)}(\mathbf{X})}{\partial \mathbf{X}} = - \left\langle \frac{\partial U_{uv}^{(np)}(\mathbf{X}, \mathbf{Y})}{\partial \mathbf{X}} \right\rangle_{np} \quad (2)$$

In other words, the nonpolar components of the mean force are obtained from an average of nonpolar forces over an ensemble of configurations generated with only nonpolar solute–solvent interactions. The polar components are obtained by subtracting these nonpolar components from the total mean forces, which are obtained from an average over an ensemble of configurations generated with full (polar and nonpolar) solute–solvent interactions.

This was implemented in the current simulation as follows: each of the eight static conformations of IFABP was solvated in a box of TIP3P water<sup>37</sup> in the presence of 150 mM NaCl. For each static conformation, two 1.05-ns 300 K molecular dynamics simulations were performed with the AMBER7 software<sup>38</sup> using the AMBER94 force field,<sup>39</sup> 2-fs time steps, SHAKE constraints,<sup>40</sup> and isobaric–isothermal conditions. One of these two MD trajectories was performed with normal solute–solvent interactions, and the other was performed with the electrostatic solute–solvent interactions turned off. To allow sufficient equilibration of the sys-

tem, only the last 1 ns of each trajectory was used for comparison of forces. Snapshots were taken every 4 ps, resulting in 250 conformations for each trajectory used in the analyses.

Explicit solvent forces were evaluated with the TINKER software package<sup>41</sup> using the AMBER94 force field.<sup>39</sup> Solvation forces were calculated by computing the total force on each atom in the presence and absence of solvent and averaging the forces over the entire trajectory. The results of these calculations from each of the trajectories are then used to obtain the components of the mean solvation force as described above.

### Implicit Solvent Forces

PB polar solvation forces were evaluated for each snapshot using APBS (<http://agave.wustl.edu/apbs/>),<sup>6</sup> which implements the force evaluation method of Im et al.<sup>24</sup> The Im et al. method uses a continuous, spline-based dielectric boundary and has been shown to give highly accurate and numerically stable forces from PB calculations. This method calculates the total solvation force as a sum of three individual terms: fixed charge (or “reaction field”) forces arising from interactions of the polarized solvent with the solute charges, dielectric boundary forces caused by the variation of the dielectric constant from solvent to the solute interior, and ionic boundary forces resulting from osmotic pressure of the ionic solution acting at the surface of the biomolecule. In the present work, the ionic boundary forces were neglected because their use with the Im et al. PB force method can cause numerical problems if incorrect parameters are used for the solvent and ion accessibility functions.<sup>42</sup> In fact, these ion boundary terms are generally accepted to be rather small<sup>23,24</sup> for low-concentration monovalent ion solutions, and generally negligible for low-charge density biomolecules.

For a useful description of the PB forces, the parameters of the underlying PB calculation must first be understood. We solved the PB equation using the APBS multigrid solver that discretizes the biomolecule on a Cartesian grid. Therefore, in addition to specifying environmental constants such as dielectric properties, ionic strength, and temperature, one must also determine the grid spacings/sizes/positions and the discretization of charges onto the grid. The majority of the calculations were performed with grids centered on the molecule with 129 grid points with grid spacings between 0.41 and 0.50 Å. Grid parameters were also varied to determine the sensitivity of the results to discretization (see below). The results of PB calculations are notoriously sensitive to the models used to describe the dielectric and ion-accessibility functions.<sup>43</sup> In the present work, we used the spline-based model of Im et al.,<sup>24</sup> which permits the efficient evaluation of *stable* solvation forces. Most calculations were performed with a 0.3 Å spline window; sensitivity of the results to this choice is discussed below. In the current calculations, we used the following environmental conditions: a temperature of 300 K, a solvent dielectric of 78.4, a protein dielectric of 2.0, and zero bulk ionic strength. The choice of protein dielectric coefficients is somewhat contentious;<sup>43–50</sup> however, a value of 2.0 is generally accepted as the appropriate choice for a biomolecular system in which dynamic behavior is treated explicitly.<sup>47,50</sup> Finally, as mentioned above, the AMBER94 force field<sup>39</sup> was used for atomic charges and radii. These sets of parameters *are not* optimized for implicit solvent calculations; however, the use of the same force field for both implicit and

explicit calculations facilitates the direct comparison between the two methods. As discussed in the conclusions, future work will determine the suitability of PB-specific force fields<sup>25,34</sup> for use in PB force calculations and the modification required to adapt existing explicit solvent force fields, such as AMBER to implicit solvation simulations.

In addition to the polar solvation forces calculated from the PB equation, we also examined the ability of the popular solvent-accessible surface area (SASA) continuum solvation model<sup>51–54</sup> to describe nonpolar contributions to solvation forces. In fact, as described by Im et al.,<sup>24</sup> evaluation of these forces arises naturally during the calculation of the PB dielectric boundary force. There is currently a wide range of parameters used in SASA nonpolar solvation models.<sup>47,51–55</sup> The per-atom forces obtained in the present calculations are evaluated with an arbitrary constant, the nonpolar coefficient (or surface tension), with a value of 105 J mol<sup>−1</sup> Å<sup>−2</sup>.

### Analysis Methods

Both the direction and magnitude of implicit and explicit solvation forces were compared. First, the magnitudes  $\|\mathbf{f}\| = \sqrt{f_x^2 + f_y^2 + f_z^2}$  of the force vectors were calculated for all atoms at each snapshot of the trajectory and the trajectory-averaged forces were correlated by least-squares fit of the data.<sup>56</sup> Second, the angle between the vectors was calculated as

$$\theta(\mathbf{f}, \mathbf{g}) = \cos^{-1} \left( \frac{\mathbf{f} \cdot \mathbf{g}}{\|\mathbf{f}\| \|\mathbf{g}\|} \right) \quad (3)$$

where  $\mathbf{f} \cdot \mathbf{g}$  denotes the dot product ( $f_x g_x + f_y g_y + f_z g_z$ ) between the two vectors. Note that, based on this definition; the maximum angle between forces is 180°. The mean of the angle between trajectory-averaged explicit and implicit forces was calculated.

## Results and Discussion

### Polar Solvation Forces

The total polar solvation forces were calculated and compared as described above. The mean force on each atom was calculated as an average over all the simulation snapshots, yielding a correlation coefficient of 0.88 over all trajectories (cf. Fig. 1A). The linear regression analysis shows that PB force magnitudes exceed explicit-solvent forces by an average factor of 2.2. In other words, while the magnitudes correlated well, the implicit solvent models systematically overestimated the solvation force and gave an average absolute error of 6.1 kJ mol<sup>−1</sup> Å<sup>−1</sup>. We also observed good agreement in the average force direction [eq. (3)] when comparing implicit and explicit solvent calculations; the average deviation angle between the two methods was 54.2° (cf. Fig. 1B).

The implicit solvent fixed charge (reaction field) force comprises, on average, 71% of the polar force magnitude and gives rise to much of the agreement between explicit and implicit polar solvation forces. The PB fixed charge forces correlate well with explicit solvent results, yielding a Pearson coefficient of 0.85. Likewise, the angle of deviation between trajectory-averaged per-atom forces is reasonable, with a mean value of 55.5°. The dielec-

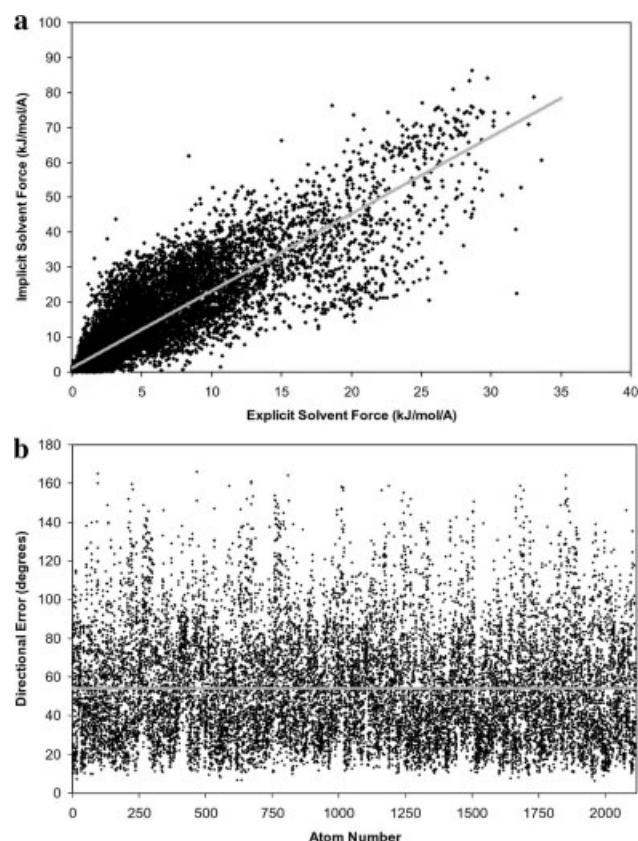


**Figure 1.** Comparison of total polar forces as calculated from the PB equation and explicit solvent methods. (a) Correlation between force magnitudes: slope, 2.2; intercept,  $1.20 \text{ kJ mol}^{-1} \text{ \AA}^{-1}$ ; correlation coefficient, 0.88. (b) Comparison of average angles between forces for each atom. The average angle between forces was 54.2 degrees.

tric boundary component constitutes the remaining 29% of the average polar solvation force. The correlation coefficient for dielectric boundary forces is significantly less than for the fixed charge component with a correlation coefficient value of 0.55. Similarly, the average angle of deviation between the two sets of forces is  $86.2^\circ$ , suggesting that the directions of the dielectric boundary forces with respect to polar explicit solvent forces is essentially random. However, when the dielectric boundary force is considered in the total polar force evaluation, the correlation coefficient rises from 0.85 to 0.88 and the relative error drops from 2.5 to 2.2, suggesting that an accurate description of this component of the force is being obtained.

#### Nonpolar Boundary Forces

The nonpolar boundary forces account for nonelectrostatic force components, and thus are not solved using the PB equation. As mentioned above, nonpolar energies are generally evaluated as the product of a nonpolar coefficient and the solvent-accessible surface area (SASA);<sup>51–54</sup> the forces arise from derivatives of the SASA with respect to atomic displacements. Many methods are available for evaluating these surface area-based energies with significant varia-

tions in the choices of SASA coefficients.<sup>47,52–55</sup> We used the spline-based method proposed by Im et al.<sup>24,25</sup> to determine SASA-based forces, with a nonpolar coefficient of  $105 \text{ J mol}^{-1} \text{ \AA}^{-2}$ .

Our calculations demonstrate that, with the current treatment of nonpolar boundary forces, there is no significant correlation between implicit and explicit solvation models (cf. Fig. 2a); the Pearson correlation coefficient is 0.28. In addition, the directions of the forces with respect to one another appear to be random, with an average directional error of  $83.2^\circ$  (cf. Fig. 2b). Nonpolar components of both explicit and implicit models are quite small, however, allowing for a good correlation between total forces. On average, the nonpolar components of explicit solvent forces comprise 10.7% of the total solvation force while the nonpolar components of implicit solvent forces comprise 13.2% of the total solvation force.

It may prove more useful to compare SASA forces to that which is needed to obtain a good correlation of total forces between models. This comparison, however, would only be advantageous after appropriate reparameterization of the PB model to reduce the systematic error obtained in the electrostatic component of forces (see Conclusions below).

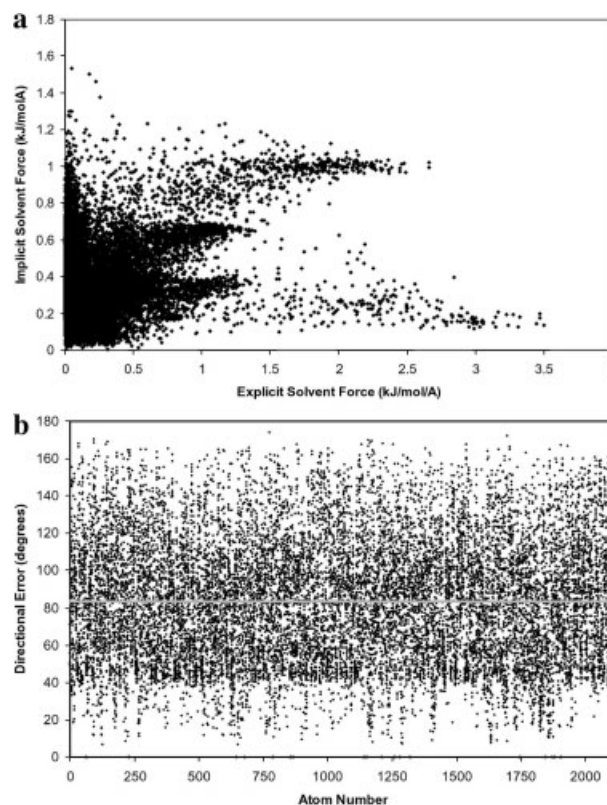


**Figure 2.** Comparison of nonpolar solvation forces as calculated for solvent-exposed IFABP atoms from the SASA model and explicit solvent methods. (a) Plot of force magnitudes. No significant correlation is observed. (b) Comparison of average angles between forces for each atom. The average angle between forces was 83.2 degrees.



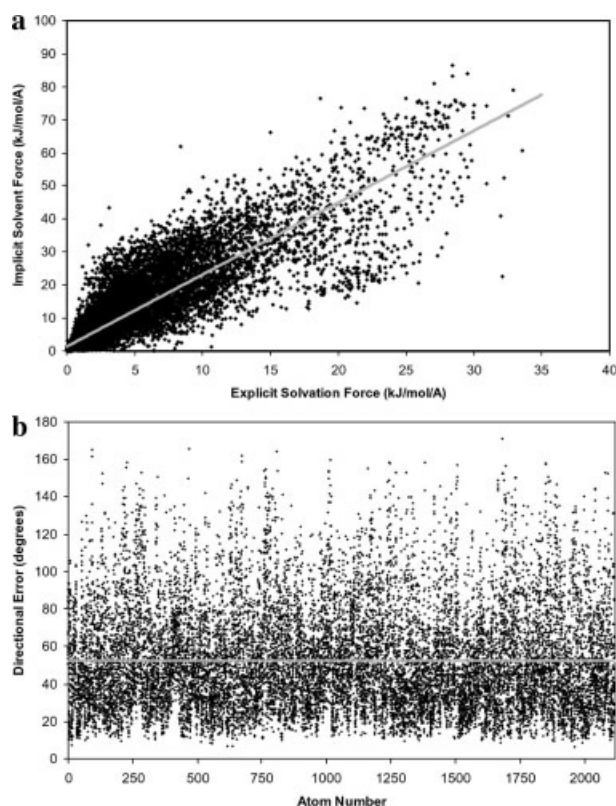


**Figure 3.** Comparison of total solvation forces as calculated from the PB equation and explicit solvent methods. (a) Correlation between force magnitudes: slope, 2.2; intercept,  $1.36 \text{ kJ mol}^{-1} \text{ \AA}^{-1}$ ; correlation coefficient, 0.88. (b) Comparison of average angles between forces for each atom. The average angle between forces was 50 degrees.

### Total Solvation Forces

In general, the nonpolar boundary forces and explicit-solvent nonpolar forces are quite small (see above), so that the accurate description of polar solvation forces by PB calculations will lead to good correlation of overall forces despite the poor description of nonpolar boundary forces. The correlation coefficient for overall forces is 0.88 with a relative error of 2.2 (cf. Fig. 3a). The directional error between forces is  $52.4^\circ$  (cf. Fig. 3b).

To assess the accuracy of forces over a range of conformations, 250 snapshots of the original IFABP trajectory with mobile solute

were used to analyze forces. The results from the mobile trajectory are very similar to those obtained from the eight static-conformation trajectories. The correlation between total forces is 0.90, with a relative error of 2.3. The directional error between total forces is  $58.7^\circ$ . These results demonstrate the ability of the PB forces to model forces over a mobile-solute trajectory as accurately as a fixed-solute trajectory.

### Sensitivity to Discretization

In the interest of efficiency, the forces from the mobile-solute trajectory were calculated with a spline window of  $0.3 \text{ \AA}$  and grid spacings of  $0.497 \times 0.486 \times 0.469 \text{ \AA}$ . However, it is important to assess the impact of grid spacing on the results, particularly the nonpolar and dielectric boundary forces. Therefore, a subset of 50 snapshots were calculated with the same grid lengths as before ( $64.1 \times 62.6 \times 60.5 \text{ \AA}$ ), but with 193 grid points in each direction, resulting in grid spacings of  $0.332 \times 0.324 \times 0.313 \text{ \AA}$ . When analyzed with respect to explicit solvent forces, the PB forces from smaller grids gave results that did not differ significantly from the results previously obtained (using larger grids). For example, when the coarser-grid and finer-grid PB forces from were correlated (using all 50 snapshots), a relative error of only 2.2% was observed with a correlation coefficient of 0.99. These results suggest that our above analyses were “converged” with respect to grid spacing.

The spline window parameter used in the PB calculations is used to smoothly discretize the dielectric and ion accessibility functions. Work by Im et al.<sup>24</sup> and Nina et al.<sup>25</sup> have suggested a number of spline windows. On the fixed-solute trajectories, we examined the sensitivity of the agreement between PB and explicit solvent forces for spline windows between 0.2 and  $1.0 \text{ \AA}$ . The results of this analysis are presented in Table 2. In general, correlations improve and relative errors decrease for smaller spline windows. However, these changes in correlation with respect to spline window are negligible with respect to the large systematic differences between PB and explicit solvent forces. Therefore, any reasonable spline window (Im et al.<sup>24</sup> suggest  $0.2\text{--}0.4 \text{ \AA}$ ) should give results with good accuracy.

### Conclusions

In the current work, we compared solvation forces calculated from explicit and implicit solvent models for snapshots obtained from explicit solvent molecular dynamics trajectories for both mobile

**Table 2.** Dependence of Explicit-PB Polar Force Correlation as a Function of Spline Window Length.

Spline window (Å)	Correlation coefficient	Avg. error in angle ( $^\circ$ )	Avg. relative error in magnitude	Avg. absolute error in magnitude ( $\text{kJ mol}^{-1} \text{ \AA}^{-1}$ )
0.2	0.88	51.6	2.0	5.4
0.3	0.88	52.4	2.2	6.0
0.4	0.87	53.7	2.4	6.9
0.5	0.87	55.4	2.6	8.0
0.6	0.86	57.3	2.9	9.4
1.0	0.81	68.2	5.0	19.8

and fixed conformations of IFABP. We showed that current implementations of the PBE are capable of generating polar solvation forces that correlate well with explicit solvent forces but systematically overestimate the magnitude of the electrostatic interactions. The results of the mobile-solute trajectory also demonstrated that the PBE is equally capable of modeling forces over a mobile-solute trajectory as a fixed-solute trajectory. SASA-based nonpolar forces, however, are found to give no significant correlation with nonpolar explicit solvent forces.

The overestimation of solvation forces with the PBE could have a number of sources. First, simple three-point water models (such as TIP3P<sup>37</sup> used in this work) have been shown to incorrectly describe the dielectric properties of bulk water<sup>57</sup> and, therefore, the effective dielectric constant of the explicit solvent simulation is somewhat different than that used in the implicit solvent calculations. Second, the relaxation properties of water near the surface of biomolecules have been shown to be dramatically different than bulk solution.<sup>46,58–61</sup> Indeed, calculation of the Kirkwood *G*-tensor<sup>62</sup> from our simulations (data not shown) indicates that the water proximal to the protein surface has significantly different dielectric characteristics than bulk water. However, the most likely suspect for the PBE overestimation is the radii parameters used for the force calculations. In particular, the spline-based dielectric boundary used in the force calculations<sup>24</sup> tends to give larger solvation energies than discontinuous “molecular surface” boundaries<sup>63</sup> when using the same atomic radii; an issue that has been addressed by appropriate reparameterization of the CHARMM force field by Nina and coworkers.<sup>25</sup> The current analysis was performed using the AMBER94 force field to provide a one-to-one correspondence between the implicit and explicit solvent results. However, as mentioned earlier, there are several force fields that have been specifically developed for PB calculations via parameterized of solvation energies obtained from experiment<sup>34</sup> and explicit solvent simulations.<sup>25</sup> The present work has illustrated that it is also possible to obtain good correlation with explicit solvation forces and thereby lays the groundwork for a more detailed parameterization of force fields based on comparisons of per-atom forces rather than global solvation energies.

## Acknowledgments

We are very grateful to Prof. Jay Ponder and Prof. Rohit Pappu for helpful discussions and the reviewers of this manuscript for useful suggestions. NAB is an Alfred P. Sloan Research Fellow.

## References

- Honig, B.; Nicholls, A. *Science* 1995, 268, 1144.
- Roux, B.; Simonson, T. *Biophys Chem* 1999, 78, 1.
- Davis, M. E.; McCammon, J. A. *Chem Rev* 1990, 94, 7684.
- Baker, N. A.; McCammon, J. A. In *Structural Bioinformatics*; Bourne, P.; Weissig, H., Eds.; John Wiley & Sons, Inc.: New York, 2003, p. 427.
- Feig, M.; Onufriev, A.; Lee, M. S.; Im, W.; Case, D. A.; Brooks, C. L. I. *J Comput Chem* 2004, 25, 265.
- Baker, N. A.; Sept, D.; Joseph, S.; Holst, M. J.; McCammon, J. A. *Proc Natl Acad Sci USA* 2001, 98, 10037.
- Lamm, G. In *Reviews in Computational Chemistry*; Lipkowitz, K. B.; Larter, R.; Cundari, T. R., Eds.; John Wiley and Sons, Inc.: Hoboken, NJ, 2003, p. 147.
- Luo, R.; Head, M. S.; Moulton, J.; Gilson, M. K. *J Am Chem Soc* 1998, 120, 6138.
- Onufriev, A.; Bashford, D.; Case, D. A. *J Phys Chem B* 2000, 104, 3712.
- Im, W.; Lee, M. S.; Brooks, C. L. I. *J Comput Chem* 2003, 24, 1691.
- Bashford, D.; Case, D. A. *Annu Rev Phys Chem* 2000, 51, 129.
- Bordner, A. J.; Huber, G. A. *J Comput Chem* 2003, 24, 353.
- Coalson, R. D.; Duncan, A. *J Chem Phys* 1992, 97, 5653.
- Davis, M. E.; McCammon, J. A. *J Comput Chem* 1989, 10, 386.
- Grant, J. A.; Pickup, B. T.; Nicholls, A. *J Comput Chem* 2001, 22, 608.
- Luo, R.; David, L.; Gilson, M. K. *J Comput Chem* 2002, 23, 1244.
- Zauhar, R. J.; Morgan, R. S. *J Mol Biol* 1985, 186, 815.
- Zhou, H. X. *Biophys J* 1993, 65, 955.
- Cortis, C. M.; Friesner, R. A. *J Comput Chem* 1997, 18, 1591.
- Holst, M.; Baker, N.; Wang, F. *J Comput Chem* 2000, 21, 1319.
- Warwicker, J.; Watson, H. C. *J Mol Biol* 1982, 157, 671.
- Sharp, K. A.; Honig, B. *J Phys Chem* 1990, 94, 7684.
- Gilson, M. K.; Davis, M. E.; Luty, B. A.; McCammon, J. A. *J Phys Chem* 1993, 97, 3591.
- Im, W.; Beglov, D.; Roux, B. *Comput Phys Commun* 1998, 111, 59.
- Nina, M.; Im, W.; Roux, B. *Biophys Chem* 1999, 78, 89.
- Davis, M. E.; McCammon, J. A. *J Comput Chem* 1990, 11, 401.
- Egolf, B.; Tavan, P. *J Chem Phys* 2004, 120, 2056.
- Friedrich, M.; Zhou, R. H.; Edinger, S. R.; Friesner, R. A. *J Phys Chem B* 1999, 103, 3057.
- Lu, Q.; Luo, R. *J Chem Phys* 2003, 119, 11035.
- Gilson, M. K. *J Comput Chem* 1995, 16, 1081.
- Dominy, B. N.; Brooks, C. L. *J Phys Chem B* 1999, 103, 3765.
- Onufriev, A.; Case, D. A.; Bashford, D. *J Comput Chem* 2002, 23, 1297.
- Feig, M.; Im, W.; Brooks, C. L. I. *J Chem Phys* 2004, 120, 903.
- Sitkoff, D.; Sharp, K. A.; Honig, B. *J Phys Chem* 1994, 98, 1978.
- Hodson, M. E.; Cistola, D. P. *Biochemistry* 1997, 36, 2278.
- Lindahl, E.; Hess, B.; van der Spoel, D. *J Mol Model* 2001, 7, 306.
- Jorgensen, W. L.; Chandrasekhar, J.; Madura, J. D. *J Chem Phys* 1983, 79, 926.
- Pearlmann, D. A.; Case, D. A.; Caldwell, J. W.; Ross, W. S.; Cheatham, T. E., 3rd; DeBolt, S.; Ferguson, D.; Seibel, G.; Kollman, P. *Comput Phys Commun* 1995, 91, 1.
- Cornell, W. D.; Cieplak, P.; Bayly, C. I.; Gould, I. R.; Merz, K. M.; Ferguson, D. M.; Spellmeyer, D. C.; Fox, T.; Caldwell, J. W.; Kollman, P. A. *J Am Chem Soc* 1996, 118, 2309.
- Ryckaert, J.-P.; Ciccotti, G.; van Gunsteren, W. F. *J Comput Phys* 1977, 23, 327.
- Ponder, J. W.; Washington University in St. Louis: St. Louis, MO, 2003.
- Personal communication: Swanson, J. M. J.; McCammon, J. A. MM/PBSA calculations with APBS using nonzero ionic strengths has been shown to lead to unrealistically large energies when incompatible spline-based characteristic functions are used to describe the dielectric coefficient and the ion accessibility. 2004.
- Dong, F.; Vijaykumar, M.; Zhou, H. X. *Biophys J* 2003, 85, 49.
- Mertz, E. L.; Krishtalik, L. I. *Proc Natl Acad Sci USA* 2000, 97(5), 2081–2086.
- Sharp, K.; Jeanecharles, A.; Honig, B. *J Phys Chem* 1992, 96, 3822.
- Simonson, T. *Int J Quantum Chem* 1999, 75, 45.
- Elcock, A. H.; Sept, D.; McCammon, J. A. *J Phys Chem B* 2001, 105, 1504.

48. Roux, B. In *Computational Biochemistry and Biophysics*; Becker, O. M.; MacKerell, A. D. J.; Roux, B.; Watanabe, M., Eds.; Marcel Dekker: New York, 2001, p. 133.
49. Nielsen, J. E.; Andersen, K. V.; Honig, B.; Hooft, R. W. W.; Klebe, G.; Vriend, G.; Wade, R. C. *Protein Eng* 1999, 12, 657.
50. Sham, Y. Y.; Muegge, I.; Warshel, A. *Biophys J* 1998, 74, 1744.
51. Herman, R. B. *J Phys Chem* 1972, 76, 2754.
52. Chothia, C. *Nature* 1974, 248, 338.
53. Sharp, K. A.; Nicholls, A.; Fine, R. F.; Honig, B. *Science* 1991, 252, 106.
54. Wesson, L.; Eisenberg, D. *Protein Sci* 1992, 1, 227.
55. Sitkoff, D.; Sharp, K. A.; Honig, B. *Biophys Chem* 1994, 51, 397; discussion 404.
56. Press, W. H.; Teukolsky, S. A.; Vetterling, W. T.; Flannery, B. P. *Numerical Recipes in C*; Cambridge University Press: New York, 1992.
57. Höchtel, P.; Boresch, S.; Bitomsky, W.; Steinhäuser, O. *J Chem Phys* 1998, 109, 4927.
58. Bhattacharyya, S. M.; Wang, Z.-G.; Zewail, A. H. *J Phys Chem B* 2003, 107, 13218.
59. Lin, J.-H.; Baker, N. A.; McCammon, J. A. *Biophys J* 2002, 83, 1374.
60. Russo, D.; Hura, G.; Head-Gordon, T. *Biophys J* 2004, 86, 1852.
61. Ford, R. C.; Ruffle, S. V.; Ramirez-Cuesta, A. J.; Michalarias, I.; Beta, I.; Miller, A.; Li, J. *J Am Chem Soc* 2004, 126, 4682.
62. Allen, M. P.; Tildesley, D. J. *Computer Simulation of Liquids*; Clarendon: Oxford, 1987.
63. Lee, B.; Richards, F. M. *J Mol Biol* 1971, 55, 379.